Inorganic Chemistry

Article

pubs.acs.org/IC

Effect of the Framework Flexibility on the Centricities in Centrosymmetric $In_2Zn(SeO_3)_4$ and Noncentrosymmetric $Ga_2Zn(TeO_3)_4$

Dong Woo Lee,[§,†] Dan-bee Bak,[§,‡] Saet Byeol Kim,[†] Jiwon Kim,[†] and Kang Min Ok*[,†]

[†]Department of Chemistry and [‡]Department of Chemistry Education, Chung-Ang University, 221 Heukseok-dong, Dongjak-gu, Seoul 156-756, Republic of Korea

Supporting Information

ABSTRACT: The solid-state syntheses, crystal structures, and characterization of two stoichiometrically similar quaternary mixed metal selenite and tellurite, $In_2Zn(SeO_3)_4$ and $Ga_2Zn(TeO_3)_4$, respectively, are reported. While $In_2Zn(SeO_3)_4$ crystallizes in the centrosymmetric monoclinic space group $P2_1/n$ (No. 14) with a = 8.4331(7) Å, b = 4.7819(4) Å, c = 14.6583(13) Å, and β = 101.684(6)°, $Ga_2Zn(TeO_3)_4$ crystallizes in the non-centrosymmetric space group $I\text{-}43d$ (No. 220) with $a = b = c$ = 10.5794(8) Å. $In_2Zn(SeO_3)_4$ exhibits a two-dimensional crystal structure consisting of distorted InO_6 octahedra, ZnO_6 octahedra, and SeO_3 polyhedra. $Ga_2Zn(TeO_3)_4$ shows a three-dimensional framework structure that is composed of GaO_4 or ZnO_4 and TeO_3 polyhedra. An effect of the framework flexibility on the space group centricity is discussed. The SHG (second harmonic generation) efficiency of noncentrosymmetric $Ga_2Zn(TeO_3)_4$, using 1064 nm radiation, is similar to that of KH_2PO_4 (KDP) and is not phase-matchable (Type 1). Complete characterizations including infrared spectroscopy and thermal analyses for the reported materials are also presented, as are dipole moment calculations.

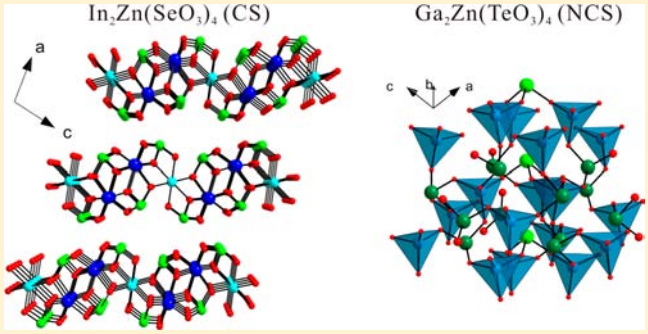

INTRODUCTION

Materials containing non-centrosymmetric (NCS) crystal structures possess a number of technologically useful characteristics such as ferroelectricity, pyroelectricity, piezoelectricity, and second-order nonlinear optical (NLO) behavior. Many synthetic chemists continuously have put forth huge efforts to develop superior performing NCS materials with the aforementioned important materials' properties.[1−7] One successful approach to increase the incidence of the crystallographic NCS structure is the introduction of polarizable cations with asymmetric coordination environment to the framework structures. With metal oxides, materials containing second-order Jahn−Teller (SOJT) distortive cations tend to exhibit a lot more of the NCS crystal structures than those found in nature.[8−13] The SOJT distortions can occur in two types of cations with asymmetric coordination environment, d^0 transition metals (Ti^{4+}, Nb^{5+}, W^{6+}, etc.) and cations with stereoactive lone pairs (Se^{4+}, Te^{4+}, I^{5+}, etc.). It has been suggested that d^{10} transition metal cations and borate groups with asymmetric π-orbital systems are other important cation groups showing a marked trend toward NCS structures.[14,15] However, it should be noted that all the local asymmetric environments are necessary, but not sufficient condition for generating NCS space group. That is, the local asymmetric units often align in an inversion relationship, leading to crystallize in crystallographic centrosymmetry (CS). Thus, it is getting much more important to understand factors controlling the space group symmetry for the rational design of NCS materials.[3,4,6] Some important elements that may contribute to determine the overall centricity are the size of metal cations and the hydrogen-bonding effect.[16−20] With these ideas in mind, we decided to investigate the Ga^{3+} (In^{3+})−Zn^{2+}−Se^{4+} (Te^{4+})−oxide system. Within the system, two classes of NCS chromophores, that is, the d^{10} transition metal (Zn^{2+}) and the SOJT distortive (Se^{4+} or Te^{4+}) cations exist. While the Zn^{2+} can exhibit polar displacement in the center of coordination environment, the lone pair cation Se^{4+} or Te^{4+} is inherently in a highly asymmetric coordination environment. In fact, a variety of zinc selenites or zinc tellurites materials have been already reported,[21−54] in which $ZnFe_2(SeO_3)_4$,[35] $Zn(TeMoO_6)$,[53] $Zn_2(MoO_4)(SeO_3)$,[54] and $Zn_2(MoO_4)(TeO_3)$[54] crystallize in NCS space groups. Here, we report solid-state syntheses and characterizations of two new quaternary mixed metal selenite and tellurite, CS $In_2Zn(SeO_3)_4$ and NCS $Ga_2Zn(TeO_3)_4$, respectively. We will demonstrate that the presence of framework flexibility caused by the introduced different p-elements such as Ga^{3+} and In^{3+} influence the framework architecture and the space group symmetry of the materials. With the NCS $Ga_2Zn(TeO_3)_4$, detailed second-harmonic generating (SHG) properties will also be reported.

Received: May 4, 2012
Published: July 2, 2012

dx.doi.org/10.1021/ic300909s | Inorg. Chem. 2012, 51, 7844−7850

EXPERIMENTAL SECTION

Reagents. ZnO (Alfa Aesar, 99%), Ga_2O_3 (Alfa Aesar, 99.9%), In_2O_3 (Alfa Aesar, 99.9%), TeO_2 (Alfa Aesar, 99.9%), and SeO_2 (Aldrich, 98%) were used as received.

Synthesis. Crystals of $In_2Zn(SeO_3)_4$ and $Ga_2Zn(TeO_3)_4$ were obtained by standard solid-state reactions. ZnO (0.814 g (1.00×10^{-3} mol)), In_2O_3 (0.278 g (1.00×10^{-3} mol)) or Ga_2O_3 (0.188 g (1.00×10^{-3} mol), and SeO_2 (0.444 g (4.00×10^{-3} mol)) or TeO_2 (0.638 g (4.00×10^{-3} mol)) were thoroughly mixed with agate mortars and pestles. The respective mixtures were introduced into fused silica tubes that were subsequently evacuated and sealed. The tubes were gradually heated to 380 °C for 5 h, and then to 600 °C (700 °C for $Ga_2Zn(TeO_3)_4$) for 48 h. The samples were cooled at a rate of 6 °C h^{-1} to room temperature. Light yellow plate crystals of $In_2Zn(SeO_3)_4$ were found with some In_2O_3 and $ZnSeO_3$. Also, light brown block crystals of $Ga_2Zn(TeO_3)_4$ were obtained along with polycrystalline sample of $Ga_2Zn(TeO_3)_4$. A pure polycrystalline sample of $In_2Zn(SeO_3)_4$ was obtained through the similar solid-state reactions. Stoichiometric amounts of ZnO, In_2O_3, and SeO_2 were thoroughly mixed and introduced into a fused silica tube, and the tube was evacuated and sealed. The tube was gradually heated to 350 °C for 5 h, 400 °C for 12 h, 450 °C for 12 h with intermediate regrindings. The powder X-ray diffraction patterns on the resultant polycrystalline products exhibited the materials were single phases and were in good agreement with the generated patterns from the single-crystal data (see the Supporting Information).

Single Crystal X-ray Diffraction. The crystal structures of $In_2Zn(SeO_3)_4$ and $Ga_2Zn(TeO_3)_4$ were determined by standard crystallographic methods. Light yellow plate crystals ($0.011 \times 0.023 \times 0.151$ mm^3) for $In_2Zn(SeO_3)_4$ and light brown block crystals ($0.026 \times 0.033 \times 0.058$ mm^3) for $Ga_2Zn(TeO_3)_4$ were used for single-crystal data analyses. All of the data were collected using a Bruker SMART BREEZE diffractometer equipped with a 1K CCD area detector, using graphite-monochromated Mo Kα radiation at 200 K. A hemisphere of data was collected using a narrow-frame method with scan widths of 0.30° in ω, and an exposure time of 5 s/frame. The first 50 frames were remeasured at the end of the data collection to monitor instrument and crystal stability. The maximum correction applied to the intensities was <1%. The data were integrated using the *SAINT* program,[55] with the intensities corrected for Lorentz factor, polarization, air absorption, and absorption attributable to the variation in the path length through the detector faceplate. A semiempirical absorption correction was made on the hemisphere of data with the *SADABS* program.[56] The data were solved and refined using *SHELXS-97*[57] and *SHELXL-97*,[58] respectively. All calculations were performed using the *WinGX-98* crystallographic software package.[59] Crystallographic data and selected bond distances for the reported material are given in Tables 1 and 2.

Powder X-ray Diffraction (XRD). The powder XRD patterns were collected on a Bruker D8-Advance diffractometer using Cu Kα radiation at room temperature with 40 kV and 40 mA. The polycrystalline samples were mounted on sample holders and scanned in the 2θ range 5−100° with a step size of 0.02°, and a step time of 1 s. The final Rietveld plots for $In_2Zn(SeO_3)_4$ and $Ga_2Zn(TeO_3)_4$ are found in the Supporting Information.

Infrared Spectroscopy. Infrared spectra were recorded on a Varian 1000 FT-IR spectrometer in the 400−4000 cm^{-1} range, with the sample embedded in a KBr matrix.

Thermogravimetric Analysis. Thermogravimetric analysis was performed on a Setaram LABSYS TG-DTA/DSC thermogravimetric analyzer. The polycrystalline samples were contained within alumina crucibles and heated at a rate of 10 °C min^{-1} from room temperature to 1000 °C under flowing argon.

Scanning Electron Microscopy/Energy Dispersive Analysis by X-ray (SEM/EDAX). SEM/EDAX has been performed using a Hitachi S-3400N/Horiba Energy EX-250 system. EDAX for $In_2Zn(SeO_3)_4$ and $Ga_2Zn(TeO_3)_4$ exhibit In/Zn/Se and Ga/Zn/Te ratios of approximately 2:1:4.

Table 1. Crystallographic Data for $In_2Zn(SeO_3)_4$ and $Ga_2Zn(TeO_3)_4$

	$In_2ZnSe_4O_{12}$	$Ga_2ZnTe_4O_{12}$
fw	802.85	907.21
space group	$P2_1/n$ (No. 14)	$I\text{-}43d$ (No. 220)
a (Å)	8.4331(7)	10.5794(8)
b (Å)	4.7819(4)	10.5794(8)
c (Å)	14.6583(13)	10.5794(8)
β (deg)	101.684(6)	90
V (Å^3)	578.87(9)	1184.09(16)
Z	2	4
T (K)	200.0(2)	200.0(2)
λ (Å)	0.71073	0.71073
ρ_{calcd} (g cm^{-3})	4.606	5.089
μ (mm^{-1})	18.640	16.245
$R(F)^a$	0.0399	0.0218
$R_w(F_o^2)^b$	0.0996	0.0483

$^aR(F) = \Sigma ||F_o| - |F_c||/\Sigma |F_o|$. $^bR_w(F_o^2) = [\Sigma w(F_o^2 - F_c^2)^2/\Sigma w(F_o^2)^2]^{1/2}$.

Second-Order Nonlinear Optical Measurements. Powder SHG measurements on polycrystalline $Ga_2Zn(TeO_3)_4$ were performed on a modified Kurtz-NLO system[60] using 1064 nm radiation. A DAWA Q-switched Nd:YAG laser, operating at 20 Hz, was used for the measurements. Because SHG efficiency has been shown to depend strongly on particle size, polycrystalline samples were ground and sieved (Newark Wire Cloth Co.) into distinct particle size ranges (20−45, 45−63, 63−75, 75−90, 90−125, >125 μm). To make relevant comparisons with known SHG materials, crystalline α-SiO_2 and $LiNbO_3$ were also ground and sieved into the same particle size ranges. Powders with particle size 45−63 μm were used for comparing SHG intensities. All the powder samples with different particle sizes were placed in separate capillary tubes. No index matching fluid was used in any of the experiments. The SHG light (i.e., 532 nm green light) was collected in reflection and detected by a photomultiplier tube (Hamamatsu). To detect only the SHG light, a 532 nm narrow-pass interference filter was attached to the tube. A digital oscilloscope (Tektronix TDS1032) was used to view the SHG signal. A detailed description of the equipment and the methodology used has been published.[61,62]

RESULTS AND DISCUSSION

Structures. *$In_2Zn(SeO_3)_4$.* $In_2Zn(SeO_3)_4$ crystallizes in the monoclinic centrosymmetric space group $P2_1/n$ (No. 14). The structure is composed of distorted InO_6 octahedra, ZnO_6 octahedra, and SeO_3 polyhedra. The unique In^{3+} and Zn^{2+} cations are coordinated by six oxygen atoms with In−O and Zn−O bond distances ranging from 2.082(5) to 2.241(5) Å and from 2.048(6) to 2.188(5) Å, respectively. The two Se^{4+} cations are connected to three oxygen atoms that form a distorted pyramidal geometry. The local asymmetric coordination environment observed in the Se^{4+} cations is attributable to their lone pairs. The Se−O bond lengths range from 1.672(5) to 1.726(5) Å.

The six-coordinate InO_6 octahedra are sharing their corners through O(4) and are forming unidimensional chains along the [010] direction (see Figure 1a). As seen in the Figure 1a, the two bridging vertices of every octahedron are in *cis* position. Then the six-coordinate ZnO_6 octahedra are linked through O(3) and O(4) and form a layered structure approximately in the *bc*-plane. (see Figure 1b). Thus, the ZnO_6 octahedra serve as interchain linkers. Interestingly, two classes of four-membered rings (4-MRs) are observed in the layer: while the one kind of 4-MRs is produced by two InO_6 and two ZnO_6

dx.doi.org/10.1021/ic300909s | *Inorg. Chem.* 2012, 51, 7844−7850

Table 2. Selected Bond Distances (Å) for $In_2Zn(SeO_3)_4$ and $Ga_2Zn(TeO_3)_4$

$In_2Zn(SeO_3)_4$				$Ga_2Zn(TeO_3)_4$	
In(1)−O(1)	2.082(5)	Se(1)−O(2)	1.672(5)	Ga(1)−O(1) × 4	1.866(5)
In(1)−O(2)	2.097(5)	Se(1)−O(4)	1.714(5)	Zn(1)−O(1) × 4	1.866(5)
In(1)−O(3)	2.138(5)	Se(1)−O(5)	1.726(5)	Te(1)−O(1) × 3	1.884(5)
In(1)−O(4)	2.175(5)	Se(2)−O(1)	1.678(5)		
In(1)−O(5)	2.209(5)	Se(2)−O(3)	1.722(5)		
In(1)−O(5)	2.241(5)	Se(2)−O(6)	1.682(6)		
Zn(1)−O(3) × 2	2.188(5)				
Zn(1)−O(4) × 2	2.165(5)				
Zn(1)−O(6) × 2	2.048(6)				

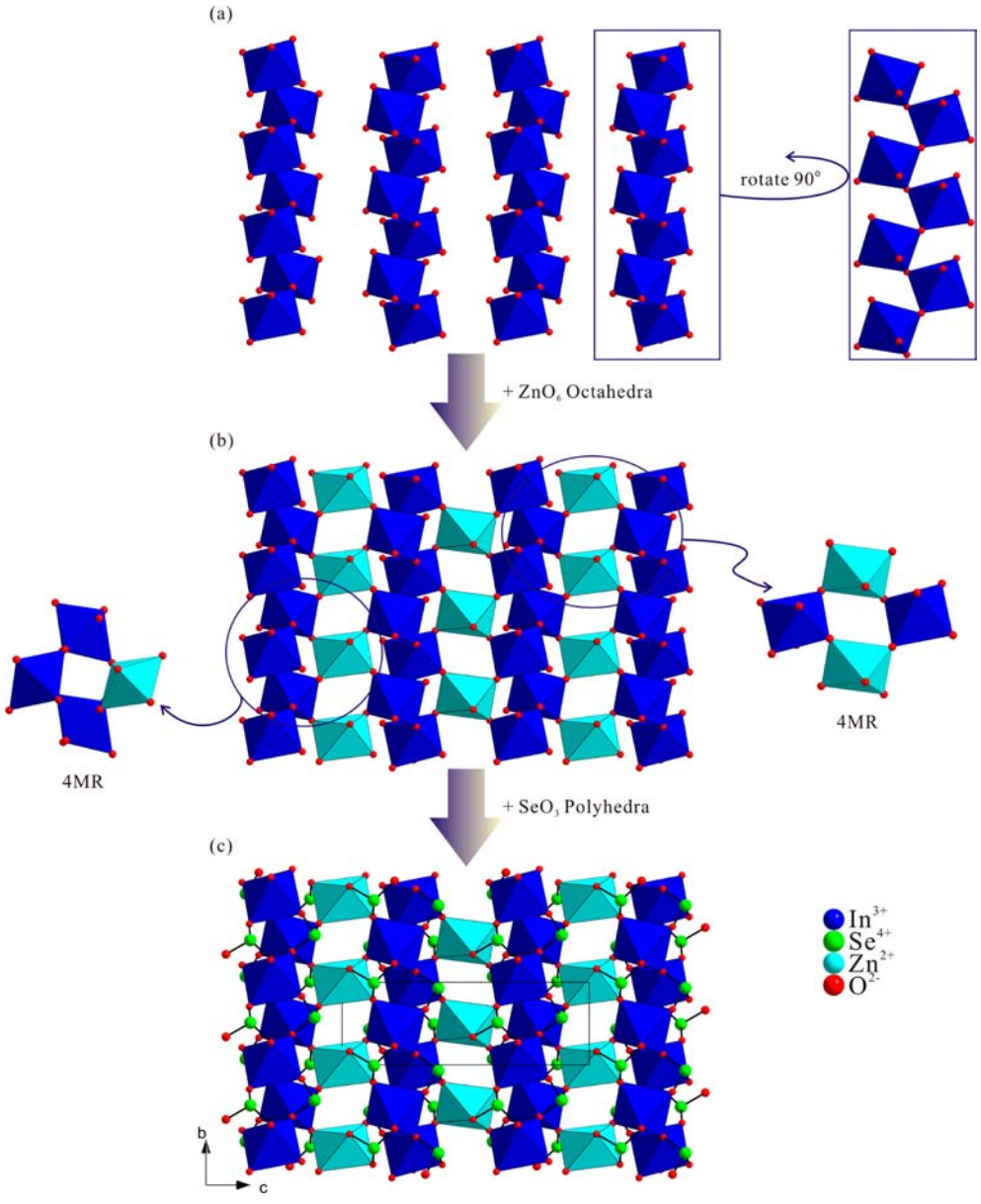

Figure 1. Ball-and-stick and polyhedral models of $In_2Zn(SeO_3)_4$ representing (a) 1D chains of corner-shared InO_6 octahedra running along the [010] direction, (b) the interchain connections by ZnO_6 octahedra to form a layered structure in the *bc*-plane, and (c) the linking of SeO_3 polyhedra to the layer.

octahedra, another type of 4-MRs is obtained by three InO_6 and one ZnO_6 octahedra. Finally, the SeO_3 polyhedra link to the layer on both sides, above and below and complete the layer (see Figure 1c). In connectivity terms, $In_2Zn(SeO_3)_4$ can be formulated as consisting of neutral layers of $\{2[In(1)O_{4/3}O_{2/2}]^{-1.667}\ [Zn(1)O_{4/3}O_{2/2}]^{-2.667}\ 2[Se(1)O_{2/3}O_{1/2}]^{+1.667}\ 2[Se(2)O_{1/3}O_{2/2}]^{+1.333}\}^0$. As seen in Figure 2, the lone pairs on Se^{4+} point toward approximate [001], [00$\bar{1}$], [100], and

dx.doi.org/10.1021/ic300909s | *Inorg. Chem.* 2012, 51, 7844−7850

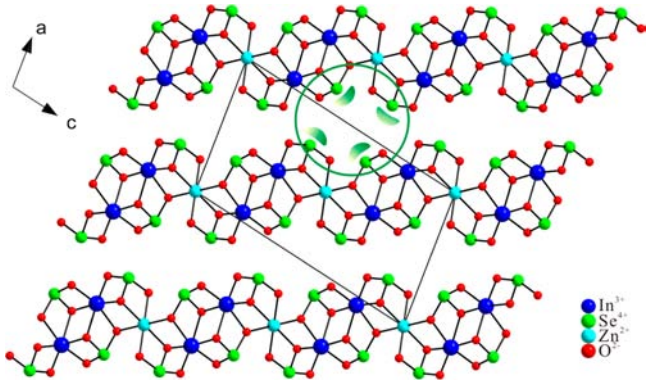

Figure 2. Ball-and-stick model of $In_2Zn(SeO_3)_4$ representing a layered structure in the *ac*-plane. Note the lone pairs on Se^{4+} point toward approximate [001], [00$\bar{1}$], [100], and [$\bar{1}$00] directions; thus, when taken as a whole, the lone pair polarization associated with Se^{4+} cancels. The lone pairs on Se^{4+} cations are drawn schematically and are not the result of the electron localization function (ELF) calculations.

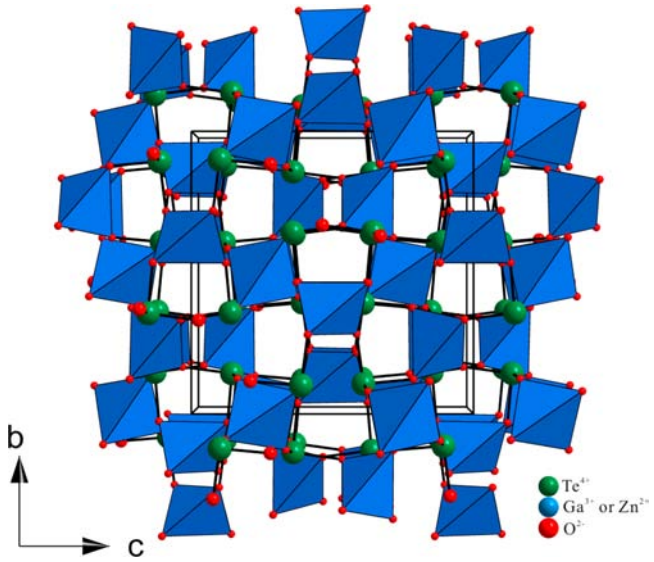

Figure 3. Ball-and-stick and polyhedral representation of $Ga_2Zn(TeO_3)_4$ in the *bc*-plane.

[$\bar{1}$00] directions; thus, when taken as a whole, the lone pair polarization associated with Se^{4+} cancels. Bond valence calculations[63,64] resulted in values 3.05, 1.91, and 4.01−4.12 for In^{3+}, Zn^{2+}, and Se^{4+}, respectively.

$Ga_2Zn(TeO_3)_4$. $Ga_2Zn(TeO_3)_4$ crystallizes in the cubic noncentrosymmetric space group *I*-43*d* (No. 220). Although the formulas are different, $Ga_2Zn(TeO_3)_4$ is isostructural to the efficient scintillators, $Bi_4(SiO_4)_3$ (BSO)[65] and $Bi_4(GeO_4)_3$ (BGO)[66] in γ-ray spectroscopy. Since there are several more examples with the similar eulytite-type structures,[67−69] a brief structural description for $Ga_2Zn(TeO_3)_4$ is given here. The reported material can be defined as a quaternary mixed metal tellurite with GaO_4 or ZnO_4 tetrahedra and TeO_3 trigonal pyramids. There is unique Ga^{3+} or Zn^{2+} cation within an asymmetric unit. The two cations Ga^{3+} and Zn^{2+} are statistically disordered over the Wyckoff position 12b sites and the occupancy of Ga^{3+}: Zn^{2+} is 2:1. The resulting formulas are in good agreement with the reported stoichiometry as well as the elemental analysis data (see the Experimental Section). The unique Ga−O or Zn−O bond length is 1.866(5) Å. The unique Te^{4+} cation is in a trigonal pyramidal environment, bonded to three oxygen atoms. The three Te−O bond distances are 1.884(5) Å. The Te^{4+} cation is in asymmetric coordination environment attributable to the stereoactive lone pair.

As can be seen in Figure 3, the structure of $Ga_2Zn(TeO_3)_4$ may be described as a three-dimensional framework that consists of corner-shared GaO_4 or ZnO_4 tetrahedra and TeO_3 polyhedra. The GaO_4 or ZnO_4 tetrahedra share their corners through O(1) with four TeO_3 groups. The TeO_3 polyhedra are linked to three Ga/ZnO_4 tetrahedra. Thus, the structure of $Ga_2Zn(TeO_3)_4$ may be described as a neutral framework of $\{2[Ga(1)O_{4/2}]^{-1}\ [Zn(1)O_{4/2}]^{-2}\ 4[Te(1)O_{3/2}]^{+1}\}^0$. Bond valence calculations[63,64] for the Ga^{3+}, Zn^{2+}, and Te^{4+} result in values 3.11, 1.93, and 3.86, respectively.

Infrared Spectroscopy. The infrared spectra of $In_2Zn(SeO_3)_4$ and $Ga_2Zn(TeO_3)_4$ exhibit bands attributable to the In−O, Zn−O, Ga−O, Se−O, and Te−O vibrations. Te−O and Se−O vibrations are observed around 744−748 and 808−844 cm^{-1}. Bands occurring about 536−590 cm^{-1} are attributed to Zn−O vibrations. Also, vibrational bands for In−O and Ga−O are observed at 430 and 688 cm^{-1}, respectively. The assignments are consistent with those of previously reported similar materials.[54,69,70] The infrared spectra for the reported materials are deposited in the Supporting Information.

Thermal Analysis. The thermal behaviors of the reported materials have been investigated using thermogravimetric analysis (TGA). As indicated by the TGA diagram, $In_2Zn(SeO_3)_4$ is stable up to 450 °C. Above the temperature, decomposition occurs attributable to the sublimation of SeO_2, calculated (experimental): 55.28% (56.31%). However, $Ga_2Zn(TeO_3)_4$ exhibits much higher thermal stability. No weight loss is observed up to 800 °C. An endothermic peak is observed in the heating curve of the differential thermal analysis diagram at 800 °C, which indicates the material melts incongruently at the temperature. The thermal stability of $Ga_2Zn(TeO_3)_4$ has been also confirmed by powder XRD. As can be seen in the Supporting Information, no substantial changes in the peak position and intensity are observed in the XRD patterns up to 810 °C. The XRD patterns obtained at higher temperatures, however, show that the material decomposes to Ga_2ZnO_4 (PDF#: 71-0843).

Second-Order Nonlinear Optical (NLO) Measurements. Because $Ga_2Zn(TeO_3)_4$ crystallizes in a noncentrosymmetric space group, its second-harmonic generating properties have been investigated. Powder SHG measurements, using 1064 nm radiation, indicates that $Ga_2Zn(TeO_3)_4$ has a moderately strong SHG efficiency, equal to that of KH_2PO_4 (KDP). Once we compare the SHG intensities, $Ga_2Zn(TeO_3)_4$ exhibits stronger response than that of the famous scintillation crystal, BGO ($6 \times \alpha$-SiO_2)[60] but similar to that of α-$Ga_2(TeO_3)_3$.[69] By sieving $Ga_2Zn(TeO_3)_4$ powder into various particle sizes ranging from 20−150 μm and measuring the SHG as a function of particle size, we were able to determine the Type 1 phase-matching capabilities of the material. As seen in the Figure 4, $Ga_2Zn(TeO_3)_4$ is not phase-matchable.

Structure−Property Relationships. It would be crucial to analyze the net direction of the polarizations for the asymmetric polyhedra in order to explain the origin and magnitude of the observed SHG efficiency. In $Ga_2Zn(TeO_3)_4$, the lone pair cation, Te^{4+} may contribute significantly toward the SHG response. First, a class of TeO_3 polyhedra are aligned along the [111] direction, where all the lone pairs in the Te^{4+} cations

dx.doi.org/10.1021/ic300909s | Inorg. Chem. 2012, 51, 7844−7850

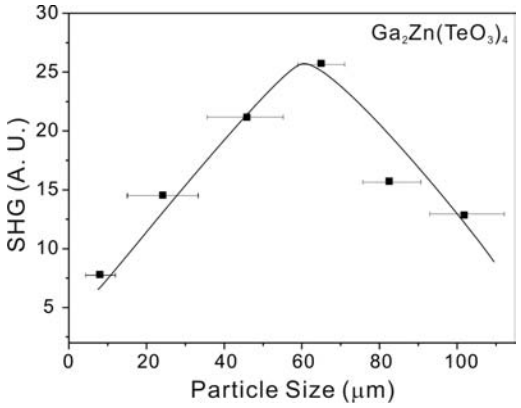

Figure 4. Phase matching curve (type 1) for $Ga_2Zn(TeO_3)_4$. The curve is to guide the eye and is not a fit to the data.

point toward [111] direction (see Figure 5a). Each TeO_3 unit has a dipole moment attributable to the different charge distribution on Te and O atoms. Since the local moment for the TeO_3 points in the opposite direction of the lone pair, a net moment in the $[\bar{1}\bar{1}\bar{1}]$ direction attributable to the alignment of the TeO_3 groups is observed. Meanwhile, a small net moment attributed to the sum of the asymmetric TeO_3 groups is also observed, where the small moment points toward [111] direction (see Figure 5b). As can be seen in Figure 5c, the GaO_4 or ZnO_4 tetrahedra are also pointing toward the $[\bar{1}\bar{1}\bar{1}]$ direction, which results in the polar crystal structure. However, the effect of the alignment of the GaO_4 or ZnO_4 tetrahedra to the SHG may be negligible; the sum of all the polar bonds in the normal tetrahedra with four same bond distances is zero, attributable to the symmetry. As we will discuss later, the local dipole moment calculations confirm that the moment for GaO_4 or ZnO_4 tetrahedra is zero. Thus, taking the moments as a whole, a net moment is observed along the $[\bar{1}\bar{1}\bar{1}]$ direction. This net moment that is arising from the alignment of asymmetric TeO_3 groups is responsible for the observed moderately strong SHG response.

To better understand the asymmetric coordination environment and the macroscopic net polarization, we did calculate the local dipole moments for Se^{4+} and Te^{4+} in $In_2Zn(SeO_3)_4$ and $Ga_2Zn(TeO_3)_4$. This approach has been described earlier with respect to metal oxy-fluoride octahedra.[71,72] We found that the local dipole moments for the SeO_3 and TeO_3 polyhedra in the reported materials are 9.09−9.50 and 11.62 D (D = Debyes), respectively. The values are consistent with those reported dipole moments for SeO_3 and TeO_3 polyhedra.[70,73−75] Also, the local dipole moments for the GaO_4 or ZnO_4 tetrahedra exhibit 0 D as expected. A complete calculation of dipole moments for the constituted polyhedra is listed in Table 3.

Table 3. Calculation of Dipole Moments for SeO_3, TeO_3, ZnO_4, and GaO_4 Polyhedra in $In_2Zn(SeO_3)_4$ and $Ga_2Zn(TeO_3)_4$

compound	species	dipole moment (D)
$In_2Zn(SeO_3)_4$	$Se(1)O_3$	9.09
	$Se(2)O_3$	9.50
$Ga_2Zn(TeO_3)_4$	$Te(1)O_3$	11.62
	$Zn(1)O_4$	0
	$Ga(1)O_4$	0

CS versus NCS Structures. Although the reported materials are stoichiometrically similar, they possess crystallographically different centricities. While $In_2Zn(SeO_3)_4$ crystallizes in the CS space group $P2_1/n$, $Ga_2Zn(TeO_3)_4$ exhibits the NCS space group, $I\text{-}43d$. With $In_2Zn(SeO_3)_4$, the In^{3+} is in a six-coordinate octahedral environment. However, the Ga^{3+} cation in $Ga_2Zn(TeO_3)_4$ possesses a four-coordinate tetrahedral geometry. The different coordination environments are consistent with the ionic radii of the cations, (In^{3+} (0.80 Å) and Ga^{3+} (0.47 Å)).[76] The larger cation, In^{3+} contains a great deal of flexibility within the framework structure. In fact, the In−O bond distances range from 2.082(5) to 2.241(5) Å with a distorted InO_6 octahedral environment. In other words, the larger In^{3+} cation can exhibit flexibility that maintains the InO_6 octahedral coordination environment through the distortions. Thus, the SeO_3 polyhedra are connected in an antiparallel manner to minimize any unfavorable repulsion of lone pairs, which renders the material a two-dimensional CS structure. In

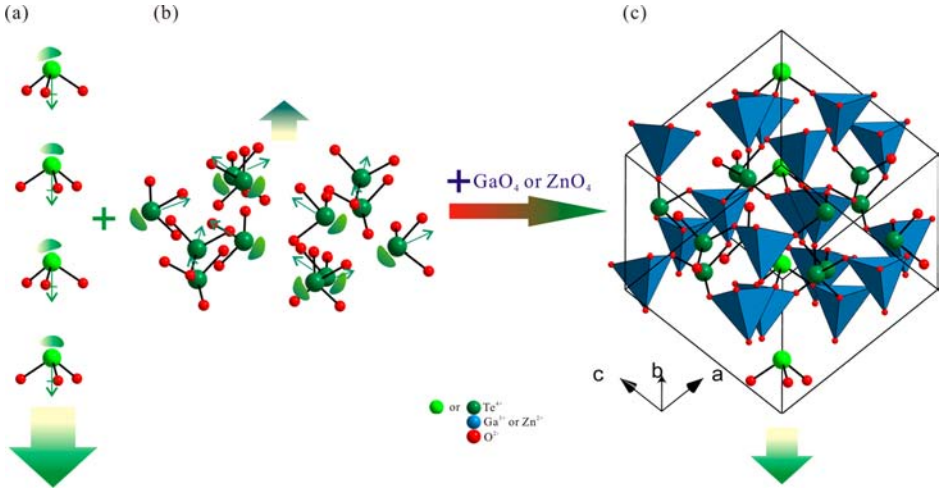

Figure 5. Ball-and-stick and polyhedral representations of $Ga_2Zn(TeO_3)_4$. A moment is observed toward the $[\bar{1}\bar{1}\bar{1}]$ direction attributable to the alignment of the TeO_3 groups. Another net moment attributed to the sum of the asymmetric TeO_3 groups is observed in the [111] direction. Once taken as a whole, a small net moment is observed along the $[\bar{1}\bar{1}\bar{1}]$direction. The lone pairs on Te^{4+} cations are drawn schematically and are not the result of the electron localization function (ELF) calculations.

dx.doi.org/10.1021/ic300909s | Inorg. Chem. 2012, 51, 7844−7850

$Ga_2Zn(TeO_3)_4$, the smaller cation, Ga^{3+} forms GaO_4 tetrahedra, in which all four Ga−O bond distances are identical (1.866(5) Å). Thus, the regular GaO_4 tetrahedra form a rigid backbone within the framework structure, which spontaneously direct the alignment of lone pairs in TeO_3 polyhedra and NCS structure.

CONCLUSIONS

We have successfully synthesized two stoichiometrically similar quaternary mixed metal selenite and tellurite materials, $In_2Zn(SeO_3)_4$ and $Ga_2Zn(TeO_3)_4$, by standard solid-state reactions. While $In_2Zn(SeO_3)_4$ is centrosymmetric with two-dimensional structure, $Ga_2Zn(TeO_3)_4$ is noncentrosymmetric with a three-dimensional framework structure. Detailed structural analyses suggest that the framework flexibility caused by the introduced p-elements with different sizes influence the crystallographic centricities of the materials. Powder SHG measurements on NCS $Ga_2Zn(TeO_3)_4$ using 1064 nm radiation, indicate the material is not phase-matchable (Type 1) with a similar SHG efficiency to that of KDP. We are in the process of synthesizing other new NCS mixed metal oxide materials and will be reporting on them shortly.

ASSOCIATED CONTENT

Supporting Information

X-ray crystallographic file in CIF format, calculated and observed X-ray diffraction patterns, thermal analysis diagrams, infrared spectra, and ORTEP drawings for $In_2Zn(SeO_3)_4$ and $Ga_2Zn(TeO_3)_4$. This material is available free of charge via the Internet at http://pubs.acs.org.

AUTHOR INFORMATION

Corresponding Author

*Phone: +82-2-820-5197. Fax: +82-2-825-4736. E-mail: kmok@cau.ac.kr.

Author Contributions

§These two authors contributed equally to this work and are co-first authors.

Notes

The authors declare no competing financial interest.

ACKNOWLEDGMENTS

This research was supported by Basic Science Research Program through the National Research Foundation of Korea (NRF) funded by Ministry of Education, Science and Technology (Grant No. 2010-0002480).

REFERENCES

(1) Bruce, D.; Wilkinson, A. P.; While, M. G.; Bertrand, J. A. *J. Solid State Chem.* **1996**, *125*, 228.
(2) Halasyamani, P. S.; Poeppelmeier, K. R. *Chem. Mater.* **1998**, *10*, 2753.
(3) Kepert, C. J.; Prior, T. J.; Rosseinsky, M. J. *J. Am. Chem. Soc.* **2000**, *122*, 5158.
(4) Maggard, P. A.; Stern, C. L.; Poeppelmeier, K. R. *J. Am. Chem. Soc.* **2001**, *123*, 7742.
(5) Evans, O. R.; Lin, W. *Acc. Chem. Res.* **2002**, *35*, 511.
(6) Hwu, S.-J.; Ulutagay-Kartin, M.; Clayhold, J. A.; Mackay, R.; Wardojo, T. A.; O'Connor, C. J.; Kraweic, M. *J. Am. Chem. Soc.* **2002**, *124*, 12404.
(7) Welk, M. E.; Norquist, A. J.; Arnold, F. P.; Stern, C. L.; Poeppelmeier, K. R. *Inorg. Chem.* **2002**, *41*, 5119.
(8) Bader, R. F. W. *Mol. Phys.* **1960**, *3*, 137.
(9) Bader, R. F. W. *Can. J. Chem.* **1962**, *40*, 1164.
(10) Pearson, R. G. *J. Am. Chem. Soc.* **1969**, *91*, 4947.
(11) Pearson, R. G. *J. Mol. Struct.: THEOCHEM* **1983**, *103*, 25.
(12) Wheeler, R. A.; Whangbo, M.-H.; Hughbanks, T.; Hoffmann, R.; Burdett, J. K.; Albright, T. A. *J. Am. Chem. Soc.* **1986**, *108*, 2222.
(13) Kunz, M.; Brown, I. D. *J. Solid State Chem.* **1995**, *115*, 395.
(14) Pan, S.; Smit, J. P.; Watkins, B.; Marvel, M. R.; Stern, C. L.; Poeppelmeier, K. R. *J. Am. Chem. Soc.* **2006**, *128*, 11631.
(15) Inaguma, Y.; Yoshida, M.; Katsumata, T. *J. Am. Chem. Soc.* **2008**, *130*, 6704.
(16) Sykora, R. E.; Ok, K. M.; Halasyamani, P. S.; Albrecht-Schmitt, T. E. *J. Am. Chem. Soc.* **2002**, *124*, 1951.
(17) Goodey, J.; Ok, K. M.; Broussard, J.; Hofmann, C.; Escobedo, F. V.; Halasyamani, P. S. *J. Solid State Chem.* **2003**, *175*, 3.
(18) Ok, K. M.; Baek, J.; Halasyamani, P. S.; O'Hare, D. *Inorg. Chem.* **2006**, *45*, 10207.
(19) Choi, M.-H.; Kim, S.-H.; Chang, H. Y.; Halasyamani, P. S.; Ok, K. M. *Inorg. Chem.* **2009**, *48*, 8376.
(20) Oh, S.-J.; Lee, D. W.; Ok, K. M. *Inorg. Chem.* **2012**, *51*, 5393.
(21) Gladkova, V. F.; Kondrashev, Y. D. *Kristallografiya* **1964**, *9*, 190.
(22) Hanke, K. *Naturwissenschaften* **1966**, *53*, 273.
(23) Hanke, K. *Naturwissenschaften* **1967**, *54*, 199.
(24) Matzat, E. *Tschermaks Mineral. Petrogr.* **1967**, *12*, 108.
(25) Meunier, G.; Bertaud, M. *Acta Crystallogr. B* **1974**, *30*, 2840.
(26) Kohn, K.; Inoue, K.; Horie, O.; Akimoto, S. *J. Solid State Chem.* **1976**, *18*, 27.
(27) Kondrashev, Y. D.; Nozik, Y. Z.; Fykin, L. E.; Shibanova, T. A. *Kristallografiya* **1979**, *24*, 586.
(28) Bensch, W.; Guenther, J. R. *Z. Kristallogr.* **1986**, *174*, 291.
(29) Hawthorne, F. C.; Ercit, T. S.; Groat, L. A. *Acta Crystallogr. C* **1986**, *42*, 1285.
(30) Semenova, T. F.; Rozhdestvenskaya, I. V.; Filatov, S. K.; Vergasova, L. P. *Mineral. Mag.* **1992**, *56*, 241.
(31) Engelen, B.; Boldt, K.; Unterderweide, K.; Baeumer, U. *Z. Anorg. Allg. Chem.* **1995**, *621*, 331.
(32) Giester, G. *Acta Chem. Scand.* **1995**, *49*, 824.
(33) Miletich, R. *Monatsh. Chem.* **1995**, *126*, 417.
(34) Engelen, B.; Baeumer, U.; Hermann, B.; Mueller, H.; Unterweide, K. *Z. Anorg. Allg. Chem.* **1996**, *622*, 1886.
(35) Giester, G. *Monatsh. Chem.* **1996**, *127*, 347.
(36) Feger, C. R.; Schimek, G. L.; Kolis, J. W. *J. Solid State Chem.* **1999**, *143*, 246.
(37) Harrison, W. T. A. *Acta Crystallogr. C* **1999**, *55*, 1980.
(38) Harrison, W. T. A.; Phillips, M. L. F. *Acta Crystallogr. C* **1999**, *55*, 1398.
(39) Harrison, W. T. A.; Phillips, M. L. F.; Stanchfield, J.; Nenoff, T. M. *Angew. Chem., Int. Ed.* **2000**, *39*, 3808.
(40) Johnston, M. G.; Harrison, W. T. A. *Inorg. Chem.* **2001**, *40*, 6518.
(41) Escamilla, R.; Gallardo Amores, J. M.; Moran, E.; Alario-Franco, M. A. *J. Solid State Chem.* **2002**, *168*, 149.
(42) Johnsson, M.; Tornroos, K. W. *Solid State Sci.* **2003**, *5*, 263.
(43) Johnsson, M.; Tornroos, K. W. *Acta Crystallogr. C* **2003**, *59*, i53.
(44) Jiang, H.; Feng, M. L.; Mao, J. G. *J. Solid State Chem.* **2006**, *179*, 1911.
(45) Johnsson, M.; Toernroos, K. W. *Acta Crystallogr. C* **2007**, *63*, i34.
(46) Nawash, J. M.; Twamley, B.; Lynn, K. G. *Acta Crystallogr. C* **2007**, *63*, i66.
(47) Spirovski, F.; Wagener, M.; Stefov, V.; Engelen, B. *Z. Kristallogr.-New Cryst St.* **2007**, *222*, 91.
(48) Alonso, J. A.; Martinez Lope, M. J.; de la Calle, C.; Munoz, A.; Moran, E.; Demazeau, G. *J. Phys. Conf. Ser.* **2008**, *121*, 032004−1.
(49) Jiang, H.; Huang, S. P.; Fan, Y.; Mao, J. G.; Cheng, W. D. *Chem.—Eur. J.* **2008**, *14*, 1972.
(50) Jiang, H.; Kong, F.; Fan, Y.; Mao, J. G. *Inorg. Chem.* **2008**, *47*, 7430.
(51) Kashi, T.; Yasiu, Y.; Moyoshi, T.; Sato, M.; Kakurai, K.; Iikubo, S.; Igawa, N. *J. Phys. Soc. Jpn.* **2008**, *77*, 084707−1.

(52) Zhang, D.; Johnsson, M. *Acta Crystallogr. E* **2008**, *64*, i26.
(53) Doi, Y.; Suzuki, R.; Hinatsu, Y.; Ohoyama, K. *J. Phys.: Condens. Matter* **2009**, *21*, 046006−1.
(54) Nguyen, S. D.; Kim, S.-H.; Halasyamani, P. S. *Inorg. Chem.* **2011**, *50*, 5215.
(55) *SAINT, Program for Area Detector Absorption Correction*, version 4.05; Siemens Analytical X-ray Instruments: Madison, WI, 1995.
(56) Blessing, R. H. *Acta Crystallogr., Sec. A: Found. Crystallogr.* **1995**, *A51*, 33.
(57) Sheldrick, G. M. *SHELXS-97, A Program for Automatic Solution of Crystal Structures*; University of Goettingen: Goettingen, Germany, 1997.
(58) Sheldrick, G. M. *SHELXL-97, A Program for Crystal Structure Refinement*; University of Goettingen: Goettingen, Germany: 1997.
(59) Farrugia, L. J. *J. Appl. Crystallogr.* **1999**, *32*, 837.
(60) Kurtz, S. K.; Perry, T. T. *J. Appl. Phys.* **1968**, *39*, 3798.
(61) Porter, Y.; Ok, K. M.; Bhuvanesh, N. S. P.; Halasyamani, P. S. *Chem. Mater.* **2001**, *13*, 1910.
(62) Ok, K. M.; Chi, E. O.; Halasyamani, P. S. *Chem. Soc. Rev.* **2006**, *35*, 710.
(63) Brown, I. D.; Altermatt, D. *Acta Crystallogr.* **1985**, *B41*, 244.
(64) Brese, N. E.; O'Keeffe, M. *Acta Crystallogr.* **1991**, *B47*, 192.
(65) Menzer, G. *Z. Kristallogr.* **1931**, *78*, 136.
(66) Milenov, T. I.; Rafailov, P. M.; Petrova, R.; Kargin, Y. F.; Gospodinov, M. M. *Mater. Sci. Eng., B* **2007**, *138*, 35.
(67) Sahoo, P. P.; Gaudin, E.; Darriet, J.; Row, T. N. G. *Mater. Res. Bull.* **2009**, *44*, 812.
(68) Hu, B.; Li, J.-R.; Feng, M.-L.; Huang, X.-Y. *Inorg. Chem. Commun.* **2010**, *13*, 789.
(69) Kong, F.; Xu, X.; Mao, J.-G. *Inorg. Chem.* **2010**, *49*, 11573.
(70) Lee, D. W.; Oh, S.-J.; Halasyamani, P. S.; Ok, K. M. *Inorg. Chem.* **2011**, *50*, 4473.
(71) Maggard, P. A.; Nault, T. S.; Stern, C. L.; Poeppelmeier, K. R. *J. Solid State Chem.* **2003**, *175*, 25.
(72) Izumi, H. K.; Kirsch, J. E.; Stern, C. L.; Poeppelmeier, K. R. *Inorg. Chem.* **2005**, *44*, 884.
(73) Kim, M. K.; Jo, V.; Lee, D. W.; Ok, K. M. *Dalton Trans.* **2010**, *39*, 6037.
(74) Lee, D. W.; Ok, K. M. *Solid State Sci.* **2010**, *12*, 2036.
(75) Oh, S.-J.; Lee, D. W.; Ok, K. M. *Dalton Trans.* **2012**, *41*, 2995.
(76) Shannon, R. D. *Acta Crystallogr.* **1976**, *A32*, 751.